JOURNAL OF MATERIALS SCIENCE 24 (1989) 3947–3955

Influence of filler particle shape on elastic moduli of PP/$CaCO_3$ and PP/$Mg(OH)_2$ composites

Part 1 *"Zero" interfacial adhesion*

J. JANČÁŘ
Research Institute of Macromolecular Chemistry, Tkalcovská 2, 656 49 Brno, Czechoslovakia

The effects of filler particle shape on the Young's and shear moduli of PP/$CaCO_3$ and PP/$Mg(OH)_2$ composites were studied in the concentration interval up to 50 vol/vol% filler. Calcium carbonate had irregular, approximately spherical particles and magnesium hydroxide had particles either in the form of hexagonal plates or micro-needles. The analysis based on the classical models together with structural observations enabled explanation of the composition dependences of elastic moduli of the blends studied. It was found that immobilization of PP matrix on the filler surface prominently influenced the values of G' and E' moduli of PP/$CaCO_3$ and PP/$Mg(OH)_2$ composites. The presence of the strongly immobilized PP with increasing geometrical anisotropy of the filler particles enabled a hyperstructure creation in the composites PP/$Mg(OH)_2$.

1. Introduction

One of the most prominent peculiarities of polymers is the ability to change the inherent physical and mechanical properties by chemical or physical modifications [1, 2]. The simplest way of physical modifications of common polymers (polyethylene, PE; polypropylene, PP) is their compounding with particulate fillers. Inorganic rigid fillers ($CaCO_3$, talc, mica, etc.) are used mostly for rigidity improvement, creep compliance and price/volume ratio reduction, while organic fillers (EPR, EPDM, etc.) are mostly used to increase toughness [3–7].

Polypropylene filled with inorganic rigid filler is a simple two-component system with a continuous matrix and dispersed rigid particles. Such materials are macroscopically isotropic when the geometry of particles is also isotropic (isometric fillers with approximately spherical particle symmetry – glass beads, $CaCO_3$, etc.). The composites with geometrically anisotropic particles (anisometric fillers with a lowered symmetry – talc, mica, short fibres, etc.) can behave either in the isotropic manner (random orientation of particles) or as an anisotropic body when the particles are in some manner aligned. In any case it is worthwhile to know the structure–property relationships in these systems, especially for the mechanical properties determining any practical use of composite materials to a considerable extent.

Elastic moduli are the most important mechanical characteristics of materials in the small deformation region. Advantageneously, elastic moduli can be considered as the average volume quantity in the relation to the structure of a composite [8]. The modulus depends on the volume fractions and inherent properties of constituents, the phase geometry of the composite, the filler particle shape and size. In the small deformation region, a presumption of perfect interfacial adhesion between the filler and matrix is commonly considered, which simplifies solving the composite elasticity problem [9]. This is why quantification of the composition dependences of elastic moduli is on a satisfactory level and existing classical models allow plausible prediction of the rigidity of binary blends [10, 11]. Unfortunately, the vast majority of these models does not take into account either the effects of the matrix immobilization or the relaxing of the classical model presumption's validity at common filler concentrations. However, the interlayer of the immobilized matrix with changed mechanical properties, compared to the formal matrix, can strongly affect the mechanical behaviour of the composite [12, 13].

In contrast to the quite well researched PP/$CaCO_3$ composites [14], no study dealing with the composition dependences of elastic moduli of PP/$Mg(OH)_2$ composites has so far been published [15]. Magnesium hydroxide becomes a very important filler which can be used as a flame retardant and smoke supressant in the blends with PP [16]. The combustion products of the PP/$Mg(OH)_2$ composites are neither toxic nor corrosive.

The values of elastic moduli of the composites with an isometric filler increase with filler volume fraction more slowly than those of the composites with randomly oriented anisometric particles. In the composites with perfectly aligned anisometric reinforcing elements, two boundary values of the elastic moduli can be reached. The highest value of the elastic modulus, M_L,

0022–2461/89 $03.00 + .12

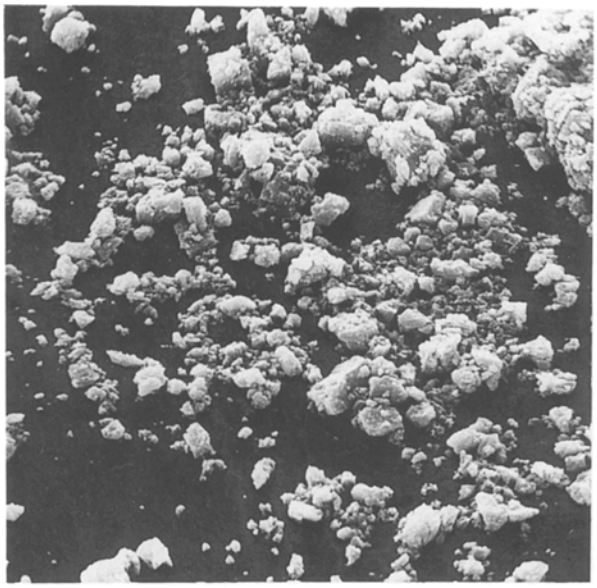

Figure 1 Scanning electron micrograph of the $CaCO_3$ grade Durcal 2 (OMYA, Switzerland) used × 799.

Figure 2 Scanning electron micrograph of the $Mg(OH)_2$ used with particles in the form of hexagonal plates (Kyowa, Japan). × 3922.

is measured parallel to the main axis of filler particles, and the lowest one, M_T, is measured perpendicular to the orientation direction. The elastic moduli, M, of the system with randomly oriented anisometric particles lie between M_L and M_T and there are many approximations which allow determination of the value of M from M_L and M_T [17, 18].

Taking into account the above arguments, our contribution pursues the following aims: ; (i) to determine and to explain effects of the filler particle shape on the elastic moduli of PP/$CaCO_3$ and PP/$Mg(OH)_2$ composites, and (ii) to investigate the applicability of existing models on the blends studied.

2. Experimental details

Commercial polypropylene Mosten 58.412 (Chemopetrol, Czechoslovakia), melt index 4 g/10 min (230° C, 21.5 N), was used as a matrix. Calcium carbonate Durcal 2 (Omya, Switzerland), magnesium hydroxide Kisuma 5B, Kisuma 7B (Kyowa, Japan) and Reachim (USSR) were used as fillers. The characteristics of the fillers used are listed in Table I. Calcium carbonate was used as-received and/or surface treated with about 1 wt/wt % of the blends of the stearic acid and calcium stearate (Fig. 1). Magnesium hydroxide was also used as-received and/or surface treated with about 2 wt/wt % of the oleic acid by the producers. Particles of $Mg(OH)_2$ Kisuma 5B and Reachim had the form of hexagonal plates (Fig. 2) and Kisuma 7B had needle-shaped particles (Fig. 3).

The components were mixed in the PLE 651 Plasticorder Brabender (the chamber W-50-H, charge 47 ml, 200° C, 50 r.p.m., 10 min). Out of compounded materials the plaques 150 mm × 150 mm × 1 mm were compression moulded at 210° C (5 min without pressure, 2 min under 6 MPa) and then cooled to 100° C min^{-1} under a pressure of 6 MPa. The specimens cut from the plaques were annealed for 1.5 h at 114° C and then slowly cooled at about 5° C min^{-1}

The measurements of the E' modulus were carried out on a dynamic mechanical thermal analyser (Polymer Laboratories, GB) and G' modulus was measured with the aid of a free oscillating torsion pendulum at 23° C, 1 Hz.

3. Results and discussion

While the Young's and shear moduli of the PP/$CaCO_3$ composites (series D2, D2-N) increased monotonically with the volume fraction of $CaCO_3$, local extremes appeared on the composition dependences of the PP/$Mg(OH)_2$ composites with both lamellar and needle-shaped particles (Figs 4, 5). The reinforcement

TABLE I Characteristics of the fillers used

Chemical nature	Grade	Specific surface area ($m^2 g^{-1}$)	Density ($g cm^{-3}$)	Youngs modulus (GPa)	Shear modulus (GPa)	Average aspect ratio, p
$CaCO_3$	Durcal 2	3.3	2.71	72	28	irregular approximately spherical $p \approx 1$
$Mg(OH)_2$	Kisuma 5B	7	2.36	64*	25*	hexagonal lamellae $p \approx 5$
	Reachim	6.8	2.36	64	25	hexagonal lamellae $p \approx 5$
	Kisuma 7B	37	2.36	64	25	needles $p \approx 25$

*The values of E and G moduli of $Mg(OH)_2$ were estimated from the relation between elastic moduli and hardness of materials

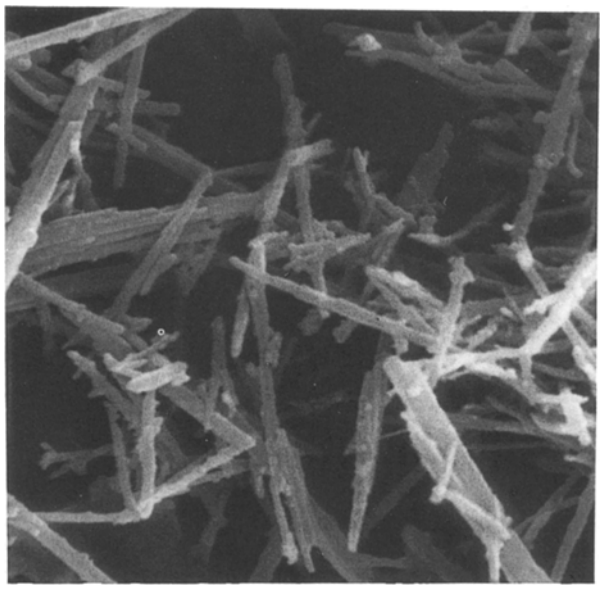

Figure 3 Scanning electron micrograph of the $Mg(OH)_2$ used with particles in the form of microfibres or needles (Kyowa, Japan). × 3922.

was the most prominent in composite with $Mg(OH)_2$ needles, but the prominency was lost for volume fractions, v_f, greater than 0.3. At the same time, our observations showed significantly higher E' and G' moduli of any systems studied which were filled with untreated fillers.

3.1. Composites PP/$CaCO_3$ with isometric particles

For analysis of the composition dependence of the PP/$CaCO_3$ composites elastic moduli, we used the Kerner–Nielsen equation [9]

$$\frac{M_c}{M_m} = \frac{1 + ABv_f}{1 - B\psi v_f} \quad (1)$$

with a semiempirical modificating function, ψ in the form

$$\psi = 1 + \frac{1 - v_f^{max}}{(v_f^{max})^2} v_f \quad (2)$$

where A, B are constants, M_c and M_m are the elastic moduli of the composites or matrix, respectively [17].

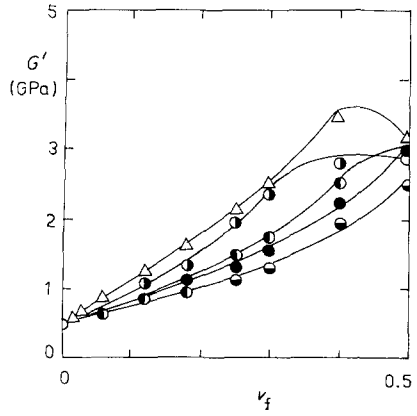

Figure 4 Concentraion dependence of the shear modulus of composites with different fillers. (△) PP/$Mg(OH)_2$ needles; (◑) PP/$Mg(OH)_2$ plates untreated; (◐) PP/$Mg(OH)_2$ plates surface-treated; (●) PP/$CaCO_3$ untreated; (◒) PP/$CaCO_3$ surface-treated.

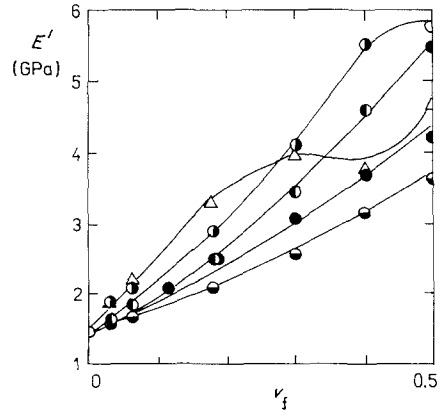

Figure 5 Concentration dependence of the Young's E' modulus of composites with different fillers. Symbols as in Fig. 4.

For the PP/$CaCO_3$ composites, $A = 1.17$, $B = 0.956$ for Youngs modulus and 0.961 for the shear modulus. A further way in which to modify Equation 1 is the incorporation of the term "apparent filler volume fraction", v_{fa}, for example in the form [13]

$$v_{fa} = (1 + b)v_f \quad (3)$$

in which b denotes the extent of the interlayer.

Taking into account random close packing of $CaCO_3$ particles, we used the value of maximum volume fraction of filler, v_f^{max}, for both series D2 and D2-N equal to 0.637 [17]. Equation 1 then gave quite good accordance between theoretical and experimental values of elastic moduli (Figs 6, 7) of PP/$CaCO_3$ composite with surface-coated filler. The same theoretical curves are very flat in comparison to experimental dependences for the PP/$CaCO_3$ composite with untreated $CaCO_3$. The discrepancy described above is probably mostly due to a worse dispersion of the surface untreated $CaCO_3$ in a nonpolar PP matrix [19] which yields the origin of filler agglomerates which is also documented by scanning electron micrographs of fracture surfaces (Fig. 8). We could neither compute nor measure the real values of v_f^{max} for both surface-treated and untreated $CaCO_3$ because of their polydispersity and creation of particle agglomerates in the course of the composite preparation.

For this reason we used, for a more satisfactory

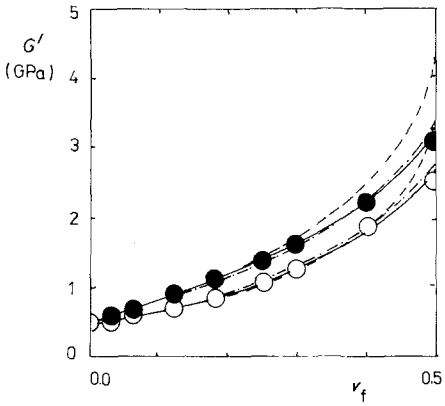

Figure 6 Comparison of the theoretical predictions based on Equation 1 and experimental values of G' modulus of PP/$CaCO_3$ composites. (●) As-received $CaCO_3$; (○) surface-treated $CaCO_3$. $f = 1$ Hz, $T = 296$ K. (– – –) Kerner–Nielsen, (—·—) Equation 5, (——) experimental data.

description of composition dependence of elastic moduli of PP/$CaCO_3$ composites, the term apparent maximum volume fraction, v_{fa}^{max} also including, except the geometrical shape of filler particles and their space packing, as v_f^{max}, the effects of interfacial interactions [13, 20]. The apparent maximum volume fraction of filler, v_{fa}^{max} was evaluated by fitting Equation 1 with the experimental dependences of elastic moduli on the volume fraction of $CaCO_3$. The lower value of $v_{fa}^{max} = 0.55$ ($v_{fa}^{max} = 0.60$ for treated $CaCO_3$) for the composite with untreated $CaCO_3$ which means a more rapid increase of moduli with v_f, is caused by a higher thermodynamic energy of adhesion, W^A, of the filler without low molecular surface treatment [21]. We conjecture that the extent of immobilized PP on the surface of the filler particles is greater than in systems PP/surface-treated $CaCO_3$ due to the more intensive interfacial interactions in the composite with higher value of W^A.

In view of the fact that immobilized molecules have lowered conformational entropy, a reduction of their molecular mobility can be supposed, which probably causes the increase in the macroscopic rigidity of the immobilized interlayer in comparison to the matrix in the bulk uninfluenced by the filler particles. The ratio between volume fraction of the formal and immobilized PP decreases with increasing v_f and that is why the experimental dependence is steeper than the theoretical one based on Equation 1 with v_f^{max}. The rate of increase of the elastic modulus, consequently, depends on the interfacial interactions, which are weaker in the composite with hydrophobic $CaCO_3$. These, together with the greater amount of immobilization of PP in agglomerates, are the main reasons for the steeper increase of elastic moduli of the system with untreated $CaCO_3$.

However, the use of Equation 1 with the fitted value of v_{fa}^{max} also gives rise to discrepancies between theoretical and experimental composition dependences of elastic moduli in the higher volume fraction region ($v_f > 0.2$). Partly, the increase of this difference with volume fraction of $CaCO_3$ can be attributed to the rising number of voids which exist on the PP–$CaCO_3$ interface and which are caused by a greater wettability of the high energy $CaCO_3$ surface by nonpolar PP. This idea is supported by measurements of the composite's density (Table II), which is always lower than that calculated from the data of the composite's chemical analysis. In spite of the larger number of voids in the composite with the untreated $CaCO_3$ the values of its elastic moduli also increase relatively fast in the high-volume fraction region. This fact is probably the consequence of a very important influence of PP matrix immobilization on the mechanical response in the small deformation region.

We reached closed theoretical approximation of experimental data of both Young's and shear moduli over the whole concentration region studied considering

TABLE II The composite density

Filler	Filler volume fraction	Surface treatment	Measured density ($g\,cm^{-3}$)	Calculated* density ($g\,cm^{-3}$)	Weight content [wt/wt %] of voids
$CaCO_3$	0.06	0.5 wt/wt %	1.013	1.014	0.010
	0.12	stearic acid	1.109	1.113	0.020
	0.18	+	1.218	1.221	0.022
	0.30	0, 3 wt/wt %	1.320	1.365	0.026
	0.40	calcium	1.566	1.600	0.029
	0.50	stearate	1.722	1.771	0.032
$CaCO_3$	0.06		1.010	1.013	0.011
	0.12		1.105	1.113	0.021
	0.18	–	1.218	1.220	0.022
	0.30		1.335	1.372	0.026
	0.40		1.600	1.612	0.021
	0.50		1.718	1.771	0.034
$Mg(OH)_2$ plates	0.06		0.981	0.985	0.009
	0.12	~2 wt/wt %	1.069	1.072	0.011
	0.18	of oleic	1.143	1.152	0.023
	0.30	acid by	1.283	1.312	0.029
	0.40	producer	1.428	1.465	0.037
	0.50		1.540	1.582	0.041
$Mg(OH)_2$ plates	0.06		0.985	0.980	0.000
	0.12		1.065	1.070	0.011
	0.18	–	1.149	1.152	0.010
	0.30		1.301	1.313	0.013
	0.40		1.434	1.470	0.027
	0.50		1.561	1.620	0.049
$Mg(OH)_2$ needles	0.06		0.990	0.992	0.008
	0.12	~2 wt/wt %	1.058	1.065	0.012
	0.18	of oleic	1.119	1.152	0.031
	0.30	acid by	1.270	1.331	0.037
	0.40	producer	1.438	1.488	0.035
	0.50		1.514	1.618	0.059

*The values of density were calculated from the results of the quantitative chemical analysis of composites studied

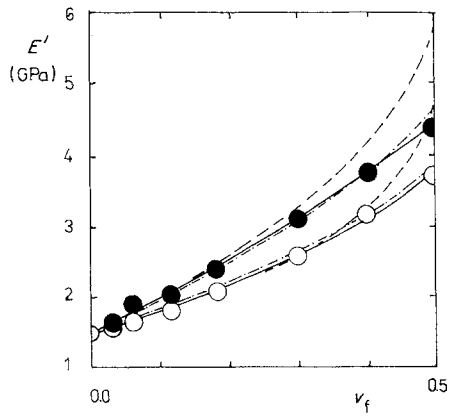

Figure 7 Comparison of the theoretical predictions based on Equation 1 and experimental values of E' modulus of PP/$CaCO_3$ composites. Details and symbols as in Fig. 6.

explicit immobilization of PP in the interlayer on the filler surface and also in agglomerates of filler particles [22]. The simplest way is an incorporation of the term apparent filler volume fraction, v_{fa}, into the Kerner–Nielsen Equation 1, considering the apparent maximum filler volume fraction, v_{fa}^{max}, equal to 1 ($\psi = 1$). We also used other simplifying assumptions: (i) the elastic modulus of immobilzed PP and filler are equal; (ii) if the value $v_{fa}^{max} = 1$ is reached, all polymer is immobilized. We have

$$v_{fa}^{max} = v_f^{max} + v_i = 1 \quad (4)$$

$$\frac{M_c}{M_m} = \frac{1 + ABv_{fa}}{1 - Bv_{fa}} \quad (5)$$

where $v_i = (bv_f)$ is the volume fraction of immobilized matrix and other symbols have the same meaning and values as in Equations 1 to 3. Fitting the experimental data by Equation 5, under the assumptions given above, we obtained reasonable values of the parameter b of Equation 3. The values of b for composites with both untreated and surface-treated $CaCO_3$ are greater when fitting data of the shear modulus, G', than that of Youngs modulus, E' (Table III). This

TABLE III The values of parameter b in Equation 3*

Filler		Fitted quantity	
		Young's modulus	shear modulus
$CaCO_3$	as-received	0.35	0.70
$CaCO_3$	surface-treated	0.08	0.60
$Mg(OH)_2$ plates	as-received	0.40	0.80
$Mg(OH)_2$ plates	surface-treated	0.15	0.65
$Mg(OH)_2$ needles	surface-treated	0.40	0.80

*The values of b were obtained by fitting the experimental results with theoretical predictions given by Equations 5, 7 and 6

distinctness is probably the consequence of an unlike geometrical mode of loading which is connected with a different susceptibility to the effects of the matrix immobilization. We suppose higher sensitivity of the shear mode loading, when only angles are changed, because of the mechanical response of both polymer immobilized in the interlayer and into the filler particles agglomerates. In the tensile arrangement, with changing volume of element unit, probably only the matrix immobilized in the interlayer gives the contribution to the mechanical response. Unfortunately, no theory takes into account seriously the effects of the geometrical arrangement on measurements of different kinds of elastic moduli.

It can be concluded that differences in the mechanical response between series D2 and D2-N with treated and untreated $CaCO_3$ is the consequence of the low molecular weight surface treatment of $CaCO_3$ which yields only a better wettability of the filler surface by PP [19]. This difference can be explained with the aid of existing models with the modified meaning of either the maximum volume fraction of filler or the volume fraction of filler. Consideration of interfacial interactions makes them apparent (v_{fa}^{max}, b). Surface treatment of $CaCO_3$ by stearic acid and calcium stearate decreases a surface energy of filler which gives better dispersion of $CaCO_3$ in PP (higher value v_{fa}^{max} – flatter composition dependence of moduli). Calcium carbonate

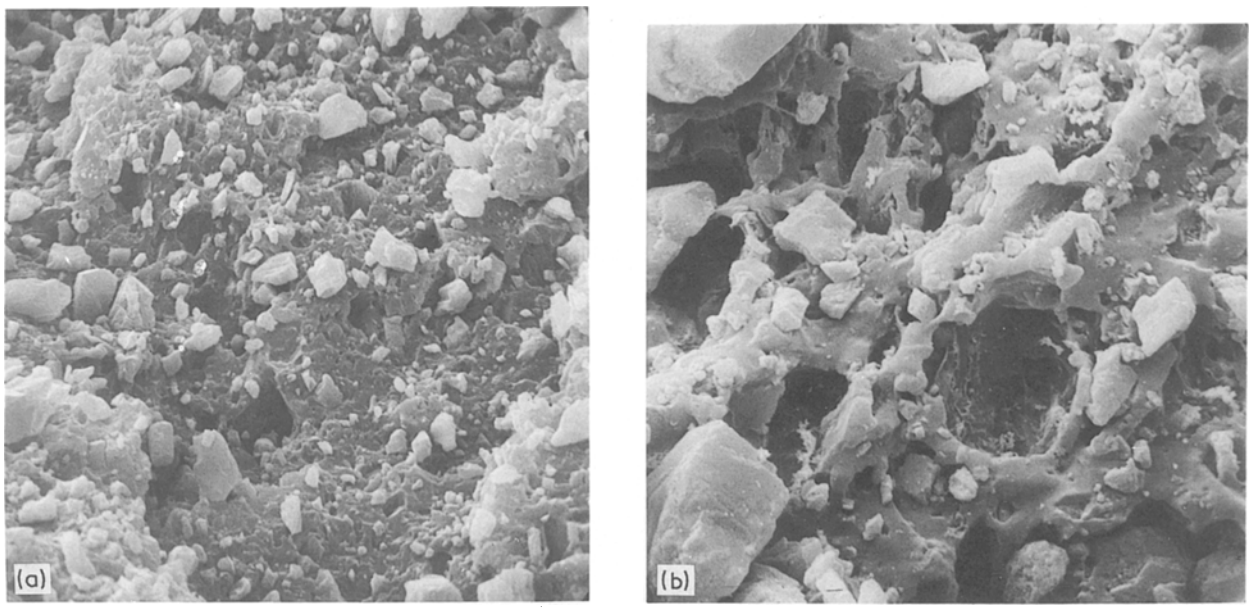

Figure 8 Scanning electron micrographs of the fracture surface of PP/$CaCO_3$ composites at $v_f = 0.2$. (a) Surface-treated $CaCO_3$, × 814, (b) as-received $CaCO_3$, × 1766.

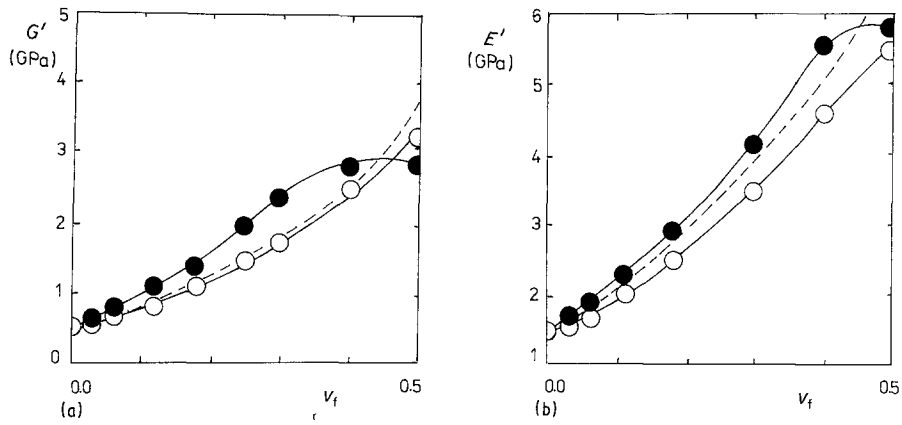

Figure 9 Comparison of theoretical predictions based on Equation 6 and experimental values of PP/$Mg(OH)_2$ plate composites. (a) G' modulus, and (b) E' modulus. f = 1 Hz; T = 296 K. (– – –); (a) Equation 6, d/h = 5. (b) Equations 6 and 7, d/h = 5; (——) Experimental data.

with a hydrophobic surface has, at the same time, lower thermodynamic energy of adhesion, W^A, which causes a smaller extent of PP immobilization and filler particle agglomeration (lower value of b).

3.2. Composites PP/$Mg(OH)_2$ with anisometric randomly oriented particles

We achieved a satisfactory accordance between the theory and experimental dependences of elastic moduli on the volume fraction of the filler for systems with both randomly oriented $Mg(OH)_2$ plates and needles using a simple Tsai approximation [6, 17]

$$M = \tfrac{3}{8} M_L + \tfrac{5}{8} M_T \quad (6)$$

M_L, M_T are parallel and perpendicular values of elastic G' and E' moduli of the composite with unidirectionally aligned reinforcing elements. For theoretical analysis of M_L and M_T we used the Halpin–Tsai equation in the form [7, 17, 18]

$$\frac{M_c^{L,T}}{M_m} = \frac{1 + A_{L,T} B_{L,T} v_f}{1 - B_{L,T} v_f} \quad (7)$$

where $A_{L,T}$ is a parameter which is given by the particle shape and the elastic modulus nature. We assessed the unpublished mechanical characteristics of $Mg(OH)_2$ available to date, considering a rough approximation and taking into account the relation between the elastic modulus and the hardness of the material. We calculated the values of Young's modulus E = 64 GPa and the shear modulus G = 25 GPa from known elastic constants of $CaCO_3$ and from a relative change in hardness between $CaCO_3$ and $Mg(OH)_2$.

There are two reasons, of a different character, causing discrepancies between theoretical and experimental composition dependences of elastic moduli of PP/$Mg(OH)_2$ composites (Figs 9, 10). Firstly, the number of voids and other defects of phase geometry increases with volume fraction of $Mg(OH)_2$, which is demonstrated by the density measurements (Table II), and secondly, the average aspect ratio of $Mg(OH)_2$ particles decreases with the volume fraction of filler due to the mechanical destruction of particles, particularly of the needle-shaped $Mg(OH)_2$. The increasing differences between calculated and measured values of the composite density with v_f is the consequence of void formation on the interface in the same manner as in PP/$CaCO_3$ composites and, to a greater extent, contrary to PP/$CaCO_3$ systems, also in the bulk of PP. The second mechanism of void formation is due to the great extent of matrix immobilization in the interlayer PP–$Mg(OH)_2$ and in the creating of clusters of filler particles which account for a matrix volume insufficiency in the bulk. The filler uninfluenced matrix cannot fill the interparticle space sufficiently and this effect is the most prominent in the composite with needle-shaped particles of $Mg(OH)_2$ because the

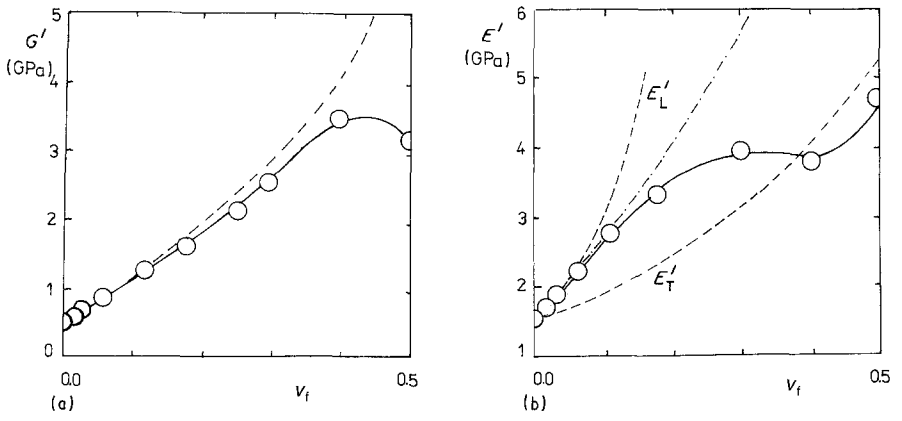

Figure 10 Comparison of theoretical predictions based on Equation 6 and experimental values of PP/$Mg(OH)_2$ plate needle composites. G' modulus, and (b) E' modulus. f = 1 Hz; T = 296 K. (— —); Equations 6 and 7, d/l = 20. (– – –): (a) Equations 6 and 7, d/l = 20; (b) Equation 6, d/l = 20. (——) Experimental data.

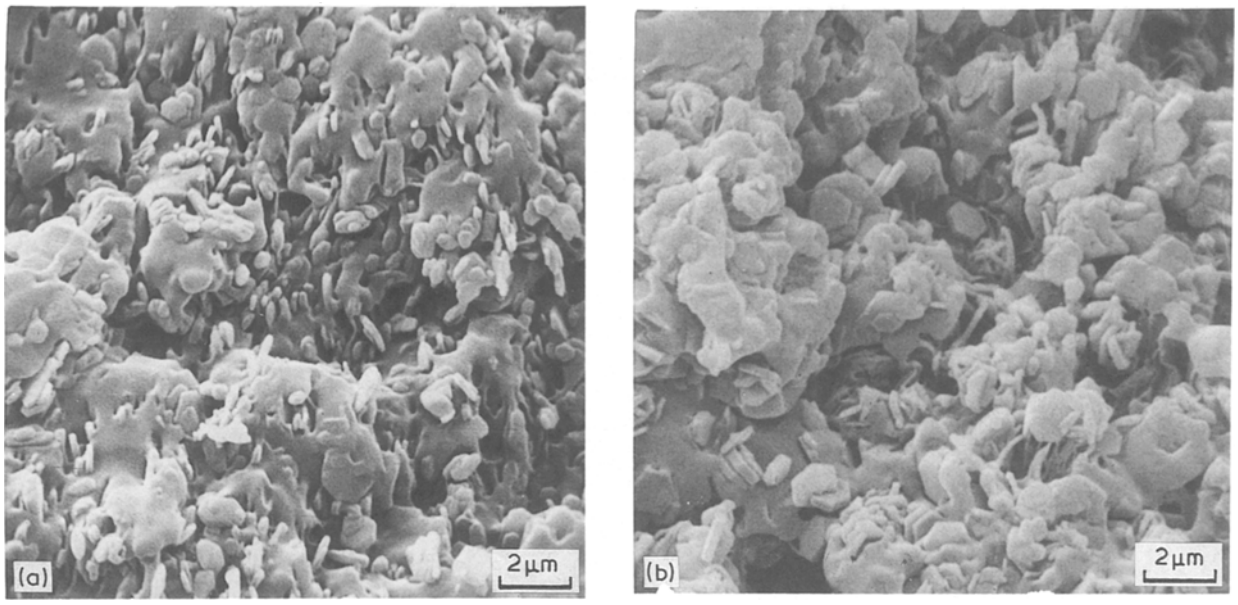

Figure 11 Scanning electron of the fracture surface in the PP/$Mg(OH)_2$ plate composites. (a) Surface-treated filler and (b) as-received filler. $v_f = 0.18$.

needles have the largest surface area and the greatest inclination towards bundles formation (Figs 11, 12).

3.3. Composites PP/$Mg(OH)_2$ with unidirectionally aligned $Mg(OH)_2$ particles

For more direct comparison of theoretical predictions based on Equation 6 with experimental data, we prepared blends with unidirectionally aligned $Mg(OH)_2$ particles and measured the longitudinal and transverse moduli E'_L and E'_T, respectively (Fig. 13). Plates of $Mg(OH)_2$ have in principle lower orientability due to the superposition of the cylindrical symmetry of the flow field and the particle shape, and therefore the simple manner of orientation used did not cause observable effects connected with a unidirectional orientation of the filler particles. Hence, values of E'_L and E'_T of the series 5B and 5B-N are practically indistinguishable and they are close to the value E' for systems with randomly oriented $Mg(OH)_2$ plates. Longitudinal and transverse moduli E'_T and E'_T of the composite containing $Mg(OH)_2$ needles show a significant difference to each other. The modulus E' of the randomly oriented composite lies between E'_L and E'_T which is in accordance with theoretical expectations. The composition dependence of the E'_T modulus can be plausibly described by the Halpin–Tsai Equation 6 in which parameter A_T is constant and independent of the aspect ratio, p, of particles ($A_T = 1/2$) [17, 18]. The increase in E'_T modulus with v_f is then of the same nature as in PP/$CaCO_3$ composites discussed above, but it is slightly steeper.

The E'_L modulus of the PP/$Mg(OH)_2$ needles composite steeply increases in the concentration region up to $v_f = 0.12$ when the aspect ratio reduction due to the mechanical destruction of needles is negligible. The concentration dependence of the E'_L modulus in this region of filler content can be plausibly described by Equation 6 with $A_L = 40$ and $B_L = 0.504$. The optimization of the aspect ratio, p, with the aid of A_L gives the value $p^{opt} = 20$ (Fig. 14). The real aspect

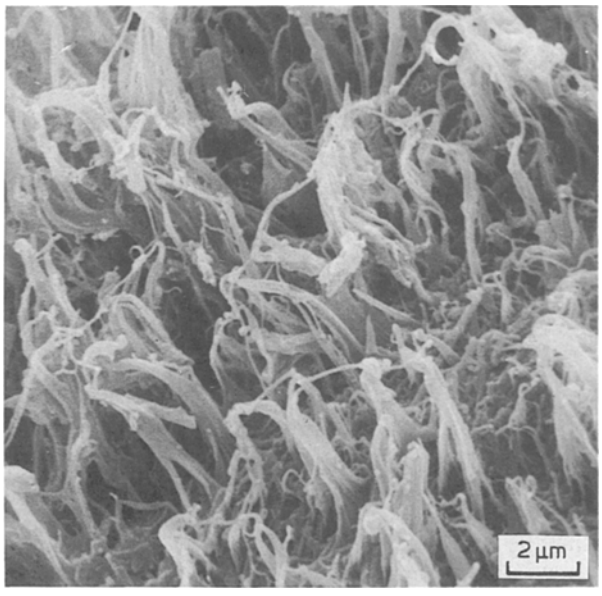

Figure 12 Scanning electron micrograph of the fracture surface of the PP/$Mg(OH)_2$ needle composite. $v_f = 0.18$.

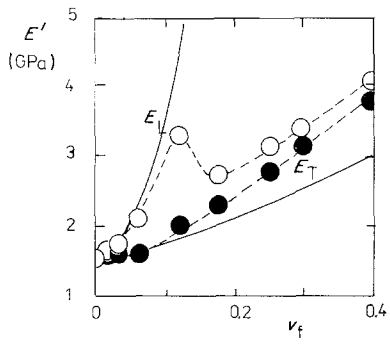

Figure 13 Concentration dependence of transverse, E'_T, and longitudinal, E'_L, moduli of the PP/$Mg(OH)_2$ needle composite with unidirectionally aligned filler particles. Curves E'_L and E'_T were calculated using the Halpin–Tsai model (Equation 6). Experimentally determined E'_L (●), experimentally determined E'_T (○). $T = 296\,K$, $f = 1\,Hz$.

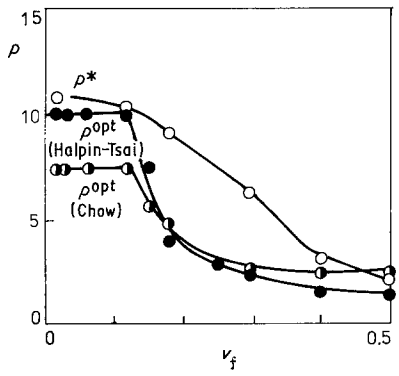

Figure 14 Concentration dependence of experimental, p^*, and optimized, p^{opt}, values of the average aspect ratio of $Mg(OH)_2$ needles. The values of p^* were obtained by the matrix extraction with decaline at 135° C. The values of p^{opt} were obtained by fitting the experimental concentration dependence of E'_L with Equation 6.

ratio of needles, p^* is reduced due to their mechanical destruction during composite preparation. The intensity of the mechanical destruction grows more intense with increasing filler volume fraction, v_f ($v_f > 0.12$) which is demonstrated by the experimental estimation of p^* by the matrix extraction in a hot decaline and consequent scanning electron micrographs of such samples. The theoretical analysis of values of E'_L with Equation 6 also leads to the opinion that the peculiarity of the mechanical response of the studied composite can be explained by proposing a hypothesis of aspect ratio apparent reduction. The values p^* and p^{opt} are very close in the region $v_f \leqslant 0.12$ while after exceeding the boundary concentration the difference between them increases steeply up to $v_f \approx 0.25$. For a filler volume fraction greater than 0.25, values p^* and p^{opt} begin to approach each other again. We based the explanation of this discrepancy on a hypothesis about a physical network formation. Consider that a physically bound space arrangement of the filler particles (the hyperstructure) has the nature of clusters or bundles of $Mg(OH)_2$ needles effectively bonded by the weak physical forces [23]. Most probably, they are the London's dispersion forces between segments of molecules adsorbed in the interpenetrating interlayers of the touching needles. The size and number of the bundles depend on the filler volume fraction, the particle aspect ratio (specific surface area) and on the manner of particle bonding. Hence the aspect ratio of the bundles, which now act as reinforcing elements and in which the individuality of the particular needles is strongly reduced, decreases. Thus, the increasing difference between p^* and p^{opt} with volume fraction, v_f, is the consequence of the increase in bundle volume fraction. However, when the hyperstructure exists in the majority of the composite bulk, the apparent decrease in aspect ratio is practically zero and p^* becomes very close to p^{opt}. The volume fraction region $0.12 \leqslant v_f \leqslant 0.25$ is probably a "transition" region in which the hyperstructure of the filler particles is created. However, we must also assume a lowering of the "effective" elastic moduli of bundles in comparison with that of $Mg(OH)_2$ needles [24]. Therefore, the value of E'_L calculated from Equation 6 also decreases with reduction in the M_f/M_m ratio at constant filler aspect ratio. This effect is comparable to that of the aspect ratio decrease at constant M_f/M_m ratio. The simple model used does not allow determination of a "measure" of the contributions of particular effects.

The effects connected with a low molecular weight surface treatment of the $Mg(OH)_2$ are qualitatively the same as in the composite $PP/CaCO_3$. The hydrophobization of the $Mg(OH)_2$ surface lowered its surface energy which led to the reduction of the wetting angle in PP and consequently to the better filler dispersion in PP. On the other hand, low molecular surface treatment causes reduction in the thermodynamic energy of adhesion, W^A, which restricts the extent of the matrix immobilization. Both these effects result in lower values of elastic moduli of the blend with surface-treated $Mg(OH)_2$.

4. Conclusions

The elastic moduli of $PP/CaCO_3$ and $PP/Mg(OH)_2$ composites with different shapes of particles increased at constant volume fraction of fillers with increasing aspect ratio and specific surface area in the sequence $CaCO_3$ < $Mg(OH)_2$ plates < $Mg(OH)_2$ needles. Under the given conditions, systems with untreated filler showed greater values of elastic E' and G' moduli due to the larger extent of the PP immobilization in the interlayer and in agglomerates. The nonmonotonic concentration dependence of E' and G' moduli of $PP/Mg(OH)_2$ composites was the consequence of both the aspect ratio, p and "effective" filler modulus, M_f, reduction. The decrease of p occurred in two parts: (i) reduction due to the mechanical destruction in the course of the composite preparation, and (ii) apparent reduction as a consequence of the hyperstructure creation. The "effective" M_f modulus of the composed reinforcing elements (bundles) was lower than that of $Mg(OH)_2$ particles due to the presence of matrix in the bundles, and weak bonding forces holding particles in the bundles.

For the $PP/CaCO_3$ composites, a plausible accordance of theoretical predictions and experimental data was achieved using the Kerner–Nielsen equation modificated by the introduction of a term for the apparent volume fraction of the filler. In addition to the pure geometrical considerations of fillers and their space packing, this term also included the matrix–filler interactions. With the aid of this term the difference between surface-treated and untreated filler of the same chemical nature could be explained as the consequence of the difference between the matrix immobilization and $CaCO_3$ dispersion.

The Halpin–Tsai equation was a plausible theoretical model for the description of the mechanical response of $PP/Mg(OH)_2$ composites. Comparison of the optimized and experimental aspect ratio of the $Mg(OH)_2$ needles gave us a chance to suggest a hypothesis about the hyperstructure of filler particle creation. Unfortunately, this simple model was not able to distinguish the "measure" of contributions of the aspect ratio and M_f reduction from the resulting composite modulus when the hyperstructure was created. The simple Tsai approximation was plausibly

used for the analysis of PP/$Mg(OH)_2$ composites with randomly oriented particles.

References

1. J. C. HALPIN, *Polym. Engng Sci.* **15** (1975) 132.
2. D. M. BIGG, *Polym. Compos.* **8** (1987) 115.
3. B. DOMINIGHAUS, *Kunstoffe* **32** (1979) 294.
4. B. PUKÁNSZKY, F. TUDOS and T. KELEN, *Polym. Compos.* **7** (1986) 106.
5. J. E. STAMHUIS, *ibid.* **5** (1984) 202.
6. J. KOLAŘÍK, G. L. AGRAWAL, Z. KRULIŠ and J. KOVA'Ř, *ibid.* **7** (1986) 463.
7. Gy. MAROSI *et al., Coll. Surf.* **23** (1986) 185.
8. Z. HASHIN, *J. Appl. Mech.* **50** (1983) 481.
9. T. B. LEWIS and L. E. NIELSEN, *J. Appl. Polym. Sci.* **14** (1970) 1449.
10. L. E. NIELSEN, *J. Compos. Mater.* **6** (1972) 136.
11. S. McGEE and R. L. McCULLOUGH, *Polym. Compos.* **2** (1981) 149.
12. P. S. THEOCARIS, Polymer NDE, Proceedings of the European Workshop on NDE of Polymers and Polymer Matrix Composites (Technomic, Lancaster, Basel, 1986).
13. JU. A. DZENIS, *Mekhanika Kompoz. Mater.* **1** (1986) 14.
14. B. PUKÁNSZKY, in "Polymer Composites", edited by B. Sedláček (de Gruyter, Berlin, 1986) p. 167.
15. S. MIYATA *J. Appl. Polym. Sci.* **25** (1980) 415.
16. P. N. HORNSBY and C. L. WATSON, *Plast. Rubb. Proc. Appl.* **6** (1986) 169.
17. L. E. NIELSEN, "Mechanical Properties of Polymers and Composites", Vol. II (Dekker, New York, 1974).
18. J. C. HALPIN and J. L. KARDOS, *Polym. Engng Sci.* **16** (1976) 344.
19. K. MITTSUISHI, S. KODAMA and H. KAWASAKI, *J. Appl. Polym. Sci.* **32** (1986) 4229.
20. K. D. ZIEGEL and A. ROMANOV, *ibid.* **17** (1973) 1119.
21. B. PUKÁNZSKY and F. TUDOS, in Proceedings of the International Conference on Interface in Polymer Composites, Cleveland, 1988 (Elsevier, New York, 1988).
22. Ju. M. TOVMASJAN, V. A. TOPOLKAREEV, V. G. OSHMJAN, A. A. BERLIN, E. F. OLEJNIK and N. S. ENIKOLOPYAN, *Vysokomol. Soed.* **A28** (1986) 321.
23. J. JANČÁŘ, J. KUČERA and P. VESELÝ, *J. Mater. Sci. Lett.*
24. J. JANČÁŘ, J. KUČERA and P. VESELÝ, to be published.

Received 22 August 1988
and accepted 11 January 1989